# Si$_2$Me$_4$-bridged zirconocene dichlorides: crystal and molecular structure of *meso*-Si$_2$Me$_4$(3-SiMe$_3$–C$_9$H$_5$)$_2$ZrCl$_2$

Odilia Pérez-Camacho [a], Sergei Ya. Knjazhanski [a,*], Gregorio Cadenas [a],
María J. Rosales-Hoz [b], Marco A. Leyva [b]

[a] *Research Center on Applied Chemistry (CIQA), Boulevard Enrique Hermocillo 140, Saltillo Coahuila, 25100 Mexico*
[b] *Research Center on Advanced Studies (CINVESTAV), Mexico DF, 07000 Mexico*

## Abstract

A series of complexes Si$_2$Me$_4$L$_2$ZrCl$_2$ (L = Ind (**1b**), 2-Me–Ind (**2b**), 3-SiMe$_3$–Ind (**3b**) and Ind–H$_4$ (**4**)) was prepared. The syntheses of **1b**, **3b** and **4** gave predominantly the *meso*-isomers, whereas a 1:1 *meso:rac* mixture was obtained for **2b**. X-ray analysis of *meso*-**3b** revealed large steric hindrance on the metal center (Cp°–Zr–Cp° is 134.6°). The 1:1 mixture of *meso*-**2b** and *rac*-**2b** (activated with MAO) produced a 2.2:1 mixture of elastic atactic and isotactic polypropylene with low activity. © 1999 Elsevier Science S.A. All rights reserved.

## 1. Introduction

The catalyst activity and the stereoselectivity in the α-olefin polymerization are influenced by changes in the structure of *ansa*-chiral metallocene catalysts such as, along with others, variation of the length and rigidity of the bridging groups [1], which affect the angle between the Cp centroids and the metal atom, and the catalyst symmetry. Among the variety of bridging groups, SiMe$_2$-bridged compounds have gained great attention because of their high activity and stereospecificity in propylene polymerizations [2]. Less attention was paid to the Si$_2$Me$_4$-bridged zirconocenes [3], which could probably combine the electron-withdrawal effect of silicon with the properties exerted by two-atom bridges [1].

We report here the synthesis and propylene polymerization tests of some Si$_2$Me$_4$-bridged *ansa*-zirconocenes, including the X-ray structure of *meso*-Si$_2$Me$_4$(3-SiMe$_3$–Ind)$_2$ZrCl$_2$.

## 2. Results and discussion

### 2.1. Synthesis of bis(indenyl)zirconocene dichlorides

The ligands **1a** and **2a** were obtained by the reaction of ClSiMe$_2$SiMe$_2$Cl with two equivalents of IndLi or 2-Me–IndLi, respectively (Scheme 1). The corresponding zirconocene dichlorides **1b** and **2b** were prepared through the in situ formation of bis-trimethyltin derivatives, which were then reacted with ZrCl$_4$ [4]. The SiMe$_3$-substituted complex **3b** was obtained through the one-pot synthesis starting from ligand **1a** (Scheme 1). The $^1$H-NMR data of the Si$_2$Me$_4$-bridged zirconocene dichlorides are summarized in Table 1.

The syntheses of Si$_2$Me$_4$(C$_9$H$_6$)$_2$ZrCl$_2$ (**1b**) and Si$_2$Me$_4$(3-SiMe$_3$–C$_9$H$_5$)$_2$ZrCl$_2$ (**3b**) gave only *meso*-isomers as hexane-insoluble and hexane-soluble fractions of the crude products, respectively. The further extraction of crude product of the synthesis of **3b** with diethyl ether, toluene and CH$_2$Cl$_2$ did not afford soluble organometallic products. The synthesis of **2b** gave a mixture of *rac* and *meso* forms in ca. 1:1 ratio. The $^1$H-NMR spectrum of **2b** (Table 1) displayed two sets

* Corresponding author.

of resonances corresponding to the *rac* and *meso* isomers, which could not be completely separated by crystallization. At best the mixture of *rac*-**2b** and *meso*-**2b** was obtained in the ratio, 75:25.

The fact of the predominant formation of *meso* isomers in our hands seems to be strange since *rac*-Si$_2$Me$_4$(C$_9$H$_6$)$_2$ZrCl$_2$ and its propene polymerization behavior have been briefly reported by Spaleck et al. [3d]. However, the detailed characterization of that complex has not been mentioned, and the compound has been assumed the *rac* form on the basis of polymerization results. To get a closer insight on the only formation of *meso* forms in the case of **1b** and **3b**, a theoretical geometry optimization of the complexes **1b**, **2b** and **3b** was performed on the semiempirical PM3(tm) basis [5]. The formation of *meso*-**1b** ($\Delta H_f = -195.910$ kcal mol$^{-1}$) and *meso*-**3b** ($\Delta H_f = -281.329$ kcal mol$^{-1}$) seems to be more favorable than the formation of *rac*-**1b** ($\Delta H_f = -195.320$ kcal mol$^{-1}$) and *rac*-**3b** ($-278.880$ kcal mol$^{-1}$). On the contrary, the formation of *rac*-**2b** ($\Delta H_f = -203.213$ kcal mol$^{-1}$) seems to be more favorable than the formation of *meso*-**2b** ($\Delta H_f = -201.586$ kcal mol$^{-1}$). It is noticeable that the difference in $\Delta H_f$ between the *rac* and *meso* forms is not so large and the standard deviation ($\delta_n = 1.22, 0.29, 0.81$, respectively) is within the method error

(see below). Thus, for the compounds **1**–**3** the formation of *rac*:*meso* mixtures should be expected. We cannot exclude a possibility of low yield formation of *rac*-**1b** which could remain in the hexane-soluble fraction. Its separation, however, was impossible. The formation of only *meso*-**3b** cannot be explained either by the synthetic method peculiarities (Scheme 1) or by any steric hindrances. It can be seen that, according to the semiempirical calculations, there is no significant difference in geometric parameters between *meso*-**3b** and *rac*-**3b** (Table 2).

Tetrahydroindenyl derivative **4** was achieved from the hydrogenation of **1b** with PtO$_2$ (dichloromethane, 25°C, 30 bar) [6]. The conversion of *meso* to *rac* form upon hydrogenation has been reported for Et(Ind)$_2$TiCl$_2$ [7]. In our case, Si$_2$Me$_4$(C$_9$H$_{10}$)$_2$ZrCl$_2$ (**4**) maintained the *meso* symmetry of its unhydrogenated precursor. The complexes **2b** and **3b** did not react under the mentioned conditions. Increasing the hydrogen pressure led to the decomposition of the both zirconocene dichlorides.

It is known that the UV or sunlight irradiation of solutions of *meso*-ethanediyl-bridged metallocenes leads to the formation of an equilibrium mixture of *meso* and *rac* forms [8]. In contrast to these, tetramethylethanediyl-bridged complexes are photostable
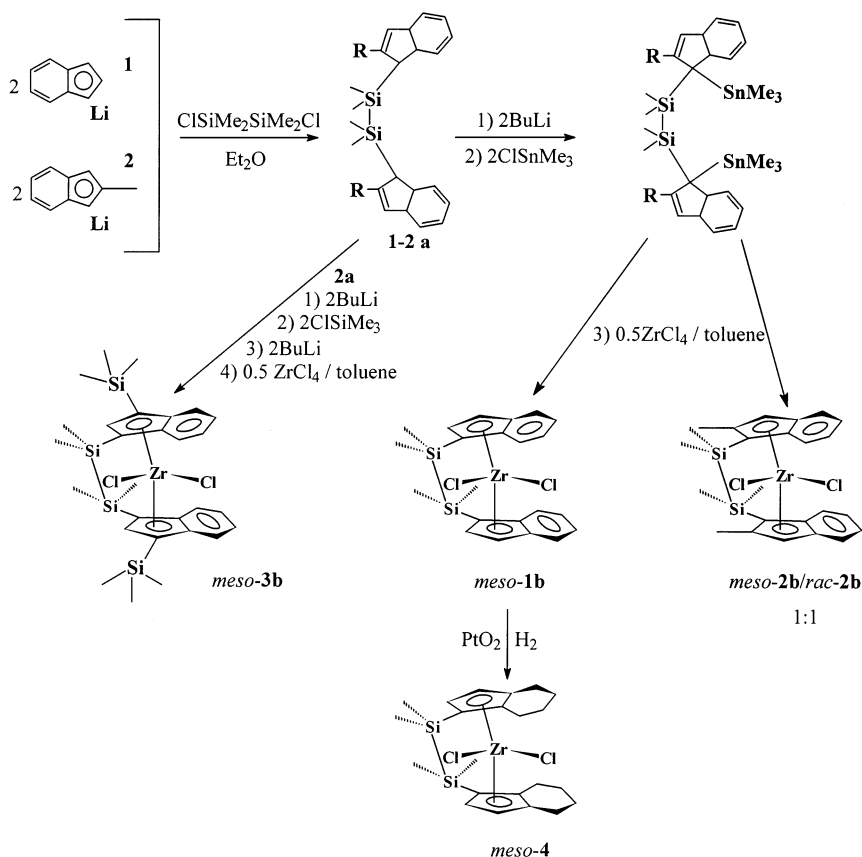


Scheme 1.

Table 1
$^1$H-NMR data of the Si$_2$Me$_4$-bridged zirconocene dichlorides (200 MHz, CDCl$_3$, 22°C, $\delta$ ppm)

| Compound | Six-membered ring | Five-membered ring | Si$_2$Me$_4$ | Substituent |
|---|---|---|---|---|
| Si$_2$Me$_4$(Flu)$_2$ZrCl$_2$ [a] | 7.79 (d, 4H, $J_{HH}$ = 8.4 Hz)<br>7.71 (d, 4H, $J_{HH}$ = 8.4 Hz)<br>7.18–7.35 (m, 8H) | | 0.91 (s, 12H) | |
| *Meso*-**1b** | 7.65 (d, 2H, $J_{HH}$ = 8.1 Hz)<br>7.45 (d, 2H, $J_{HH}$ = 8.1 Hz)<br>7.22 (t, 2H, $J_{HH}$ = 8.3 Hz)<br>7.12 (t, 2H, $J_{HH}$ = 8.4 Hz) | 6.90 (d, 2H, $J_{HH}$ = 3.2 Hz)<br>6.65 (dd, 2H, $J_{HH}$ = 3.2 Hz, and 1.0 Hz) | 0.71 (s, 6H)<br>0.59 (s, 6H) | |
| *Rac*-**1b** [b] | 7.83–7.79 (m, 2H)<br>7.71–7.67 (m, 2H)<br>7.40–7.36 (m, 2H)<br>7.27–7.22 (m, 2H) | 6.63 (d, 2H, $J_{HH}$ = 3.4 Hz)<br>6.26 (dd, 2H, $J_{HH}$ = 0.8 Hz) | 0.75 (s, 6H)<br>0.63 (s, 6H) | |
| *Meso*-**2b** | 7.75 (br d, 2H)<br>7.65 (br d, 2H)<br>7.45 (m, 2H)<br>7.00 (m, 2H) | 6.47 (s, 2H) | 0.82 (s, 6H)<br>0.72 (s, 6H) | 2.48 (s, 6H) |
| *Rac*-**2b** | 7.70 (br d, 2H)<br>7.60 (br d, 2H)<br>7.40 (m, 2H)<br>7.35 (m, 2H) | 6.60 (s, 2H) | 0.90 (s, 6H)<br>0.62 (s, 6H) | 2.09 (s, 6H) |
| *Meso*-**3b** | 7.65 (d, 2H, $J_{HH}$ = 3.1 Hz)<br>7.55 (d, 2H, $J_{HH}$ = 3.1 Hz)<br>7.10 (dd, 2H, $J_{HH}$ = 6.3, and 3.1 Hz)<br>6.90 (dd, 2H, $J_{HH}$ = 6.3, and 3.1 Hz) | 6.85 (s, 2H) | 0.72 (s, 6H)<br>0.60 (s, 6H) | 0.35 (s, 18H) |
| *Meso*-**4** | 3.0–2.75 (m, 4H)<br>2.6–2.45 (m, 4H)<br>1.70–1.4 (m, 4H)<br>1.0–0.80 (m, 4H) | 6.75 (br d, 4H)<br>6.00 (br d, 4H) | 0.12 (s, 6H)<br>0.05 (s, 6H) | |

[a] Taken from Ref. [3c]. CD$_2$Cl$_2$, 25°C.
[b] Taken from Ref. [3d].

[9]. The Si$_2$Me$_4$-bridged complexes **1b**, **3b** and **4** also appeared to be stable to sunlight, while the UV irradiation of their solutions in ether or dichloromethane led to the decomposition of the complexes.

### 2.2. Crystal structure of meso-*3b*

Single crystals of *meso*-**3b** were obtained in hexane at 0°C. The molecular structure of **3b** is shown in Fig. 1, as elucidated by an X-ray structure determination. The most relevant geometrical parameters are listed in Table 3. The structure shows the indenyl ligands disposed in a staggered conformation. The Zr–Cp° distances (2.27 and 2.24 Å), Zr–Cl distances (2.40 and 2.43 Å), Cl–Zr–Cl angle (99.18°) and the majority of the interatomic distances and angles are within the common range reported for *meso*- and *rac*-ethanediyl-bridged bis-indenylzirconium dichlorides [10]. However, the Cp°–Zr–Cp° angle (134.64°) and the dihedral angle between the Cp planes (47.8°) differ considerably from the common values (Table 4). To our knowledge, these are the most extreme values ever reported for bis-indenylzirconium dichlorides.

It is interesting to compare how the structure of **3b**

predicted by the semiempirical calculations mentioned above (Table 3) fits the structure determined by X-ray crystallography. Such comparison allows the accuracy

Table 2
Main geometric parameters, distances (Å) and angles (°) of *meso*-**2b**, *rac*-**2b**, *meso*-**3b** and *rac*-**3b** calculated by the semiempirical PM3(tm) method

| [a,b] | *Meso*-**2b** | *Rac*-**2b** | *Meso*-**3b** | *Rac*-**3b** |
|---|---|---|---|---|
| Zr–Cl | 2.425 | 2.423 | 2.435 | 2.426 |
| Zr–C(C$_5$) | 2.588 | 2.614 | 2.584 | 2.586 |
| Zr–Cp° | 2.279 | 2.312 | 2.274 | 2.278 |
| Si(1)–Si(2) | 2.473 | 2.438 | 2.470 | 2.463 |
| Cl(1)–Zr–Cl(2) | 94.25 | 93.67 | 102.45 | 97.70 |
| Cp°(1)–Zr–Cp°(2) | 133.47 | 138.58 | 132.65 | 135.34 |
| Cp°(1)–Zr–Cl(1) | 110.44 | 107.87 | 104.18 | 106.68 |
| Cp°(1)–Zr–Cl(2) | 100.97 | 100.15 | 106.48 | 102.28 |
| Cp°(2)–Zr–Cl(1) | 106.76 | 100.15 | 102.03 | 102.31 |
| Cp°(2)–Zr–Cl(2) | 103.12 | 107.94 | 105.40 | 106.66 |
| C$_{Cp}$–Si$_{SiMe3}$/Cp | – | – | 18.77 | 17.02 |
| C6/Cp | 8.59 | 8.75 | 10.02 | 9.70 |

[a] Cp°, centroid of the Cp mean plane.
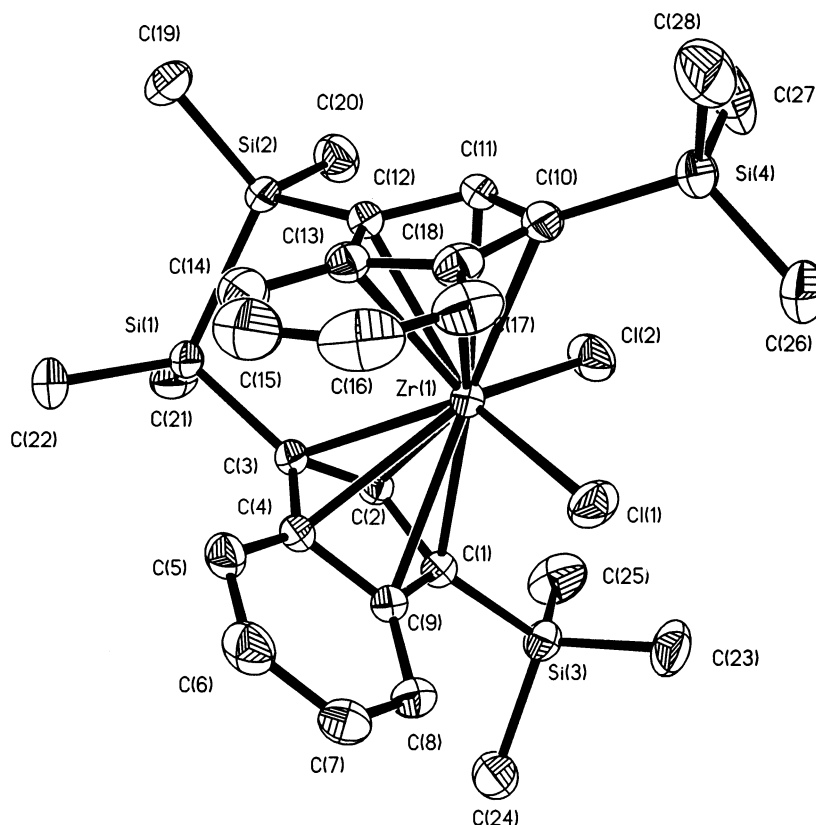[b] C6, six-membered ring.

Fig. 1. Molecular structure of *meso*-Si$_2$Me$_4$(3-SiMe$_3$–Ind)$_2$ZrCl$_2$ (**3b**).

of the calculations to be assessed. Two indenyl ligands and two Cl atoms are slightly inequivalent in the crystal structure of *meso*-**3b**, whereas the SPARTAN package does not take account of that. In fact, the inequivalence may be conditional upon the molecule packaging in the crystal and, therefore, is not considered by theoretical models that deal with isolated molecules. Although the deviations of some calculated distances and angles from the experimental ones seem to be large (namely, Zr(1)–C(13), Zr(1)–C(18), Si(1)–C(3), C(11)–C(12)–Si(2), C(4)–C(3)–Si(1)), the mean deviations are 1.68% (distances) and 1.12% (angles) for one ligand, and 0.95% (distances) and 1.96% (angles) for the other one. A somewhat larger error is observed for the bonds and angles comprising silicon atoms. For instance, the calculated distance Si(1)–Si(2) fits the experimental value with 6.05% error. This fact may be related to imprecise parametrization of silicon in the SPARTAN package [11]. The most concern is related to the accuracy of the calculation of unfixed angles. So, the deviation of the calculated Cl(1)–Zr–Cl(2) value from the experimental one is 3.30%. Also, although an 1.48% error for Cp°(1)–Zr–Cp°(2) is less than that for Zr–C distances, the 2° difference between the calculated value and experimental one does not seem negligible. In fact, the mean error of the calculations (1.77%) is less than the final R indices of the crystallographic experiment. Thus,

one may consider satisfactory the accuracy of the semiempirical calculations on zirconocene dichlorides.

The deviation of the Cp°–Zr–Cp° value from the common ones (Table 4) is obviously due to the longer length of the Si$_2$Me$_4$-bridging group compared with that of ethanediyl-bridged analogues. As a consequence, the metal center is tucked in the ligand envelope and is not accessible for the olefin coordination. As one can see from Table 4, there is no considerable difference in the Cp°–Zr–Cp° and Cp/Cp parameters between the *meso*- and the *rac*-bisindenylzirconium dichlorides. There is no significant substituent effect, either. Therefore, one may hardly expect a high polymerization activity from all Si$_2$Me$_4$-bridged *ansa*-zirconocenes. Alt [3c] and Spaleck [3d] have previously supposed a decrease in the coordination gap aperture for Si$_2$Me$_4$(Flu)$_2$ZrCl$_2$ and *rac*-Si$_2$Me$_4$(Ind)$_2$ZrCl$_2$, respectively, and confirmed the resulted obstruction for the olefin coordination by low polymerization activities of these complexes.

### 2.3. Propylene polymerization

Propylene polymerizations with the complexes **1**–**4** were performed in toluene, using MAO as activator (Al/Zr = 1000) in the temperature range from −30 to 25°C. As expected, the sterically crowded *meso*-**3b**

showed no activity while the complexes *meso*-**1b** and *meso*-**4b** presented very low activities producing oligomers of atactic polypropylene. The 1:1 mixture of *meso*-**2b** and *rac*-**2b** exhibited low oligomerization activity at 25°C. Decreasing the reaction temperature to 0°C resulted in increased overall activity (11.6 kg PP mol $Zr^{-1}$ $h^{-1}$). The extraction of crude polymer with hot heptane gave 69 wt.% of heptane-soluble atactic elastic PP ($M_n = 140\,700$, $M_w/M_n = 1.56$, $T_g = -11.2°C$) and 31 wt.% of heptane-insoluble highly crystalline isotactic PP ($M_n = 31\,100$, $M_w/M_n = 1.75$, *mmmm* = 0.95, $T_m = 155.2°C$). Supposedly, the isotactic fraction is produced by *rac*-**2b**, whereas the atactic fraction is provided by *meso*-**2b**. Generally, racemates are much more catalytically active than *meso*-isomers. The opposite behavior has been reported, for example, by Waymouth and co-workers for SiMe₂[2-Ph–Ind]₂ZrCl₂/MAO [12]. The lower activity of *rac*-**2b** is probably due to a decreased coordination gap aperture in the racemate compared to its *meso*-analog (Table 2).

The stereotactic pentade distribution (Table 5) of the heptane-soluble elastic fraction (also completely soluble in ether and pentane) matches well with the stereotactic microstructure of the ether-soluble fraction of elastic PPs reported by Waymouth and co-workers [13]. However, in contrast to the latter, the sample obtained in this work shows a very clear glass transition at −11.2°C. This difference may be attributed to the less content of isotactic segments in the polymer produced by **2b**. The detailed study on the polymerization behavior of **2b** and on the polymer properties is underway and will be reported in a separate paper.

## 3. Experimental

All operations were carried out as described in previous work from our laboratory [14]. C₅Me₄HK, indene, 2-methylindene, SiMe₃Cl, SnMe₃Cl, BuLi (hexane solution), MAO (toluene solution) were all used as purchased (Aldrich). ClSiMe₂SiMe₂Cl (Aldrich) was distilled before use, ZrCl₄ was sublimed in vacuum before use. Propene (99%) was condensed in a flask with AlEt₃ at −60°C, stirred for 2 h and then passed at ambient temperature through a column with a Na/K alloy.

NMR spectra were recorded on a Varian Gemini-200 spectrometer (200 MHz). Gel permeation chromatographic analyses were run on a Waters 150-C chromatograph in 1,2,4-trichlorobenzene at 135°C. The molecular weights of polymers were determined using polystyrene standards. Elemental analyses were performed on a Perkin–Elmer Series II CHNS/O Analyzer 2400. Analysis for zirconium and silicon were performed using an Atomic Absorption Spectrometer Varian SpectrAA-250plus.

### 3.1. X-ray analysis

C₂₈H₄₀Si₄Cl₂Zr (**3b**), a yellow prism of dimensions $0.25 \times 0.21 \times 0.19$ mm; triclinic; space group $P\bar{1}$; $a = 9.9855(8)$, $b = 10.2420(8)$, $c = 16.5327(17)$ Å; $\alpha = 91.011(7)$, $\beta = 91.012(7)$, $\gamma = 101.951(6)°$; $V = 1653.5(3)$ Å³; $Z = 2$; $D_{calc} = 1.308$ g cm⁻³; Enraf–Nonius diffractometer (Mo–K$_\alpha$; $\lambda = 0.71073$ Å); collection method $\omega - 2\theta$; absorption coefficient, 0.655 mm⁻¹; $F(000) =$

Table 3
Experimental (Exp) and calculated (SE) main bond lengths (Å) and angles (°) for *meso*-Si₂Me₄(3-SiMe₃Ind)₂ZrCl₂ (**3b**)

|  | Exp | SE |  | Exp | SE |
|---|---|---|---|---|---|
| *Bond lengths* [a] |  |  |  |  |  |
| Zr(1)–Cl(1) | 2.4019(8) | 2.433 | Zr(1)–Cl(2) | 2.4302(8) | 2.437 |
| Zr(1)–C(10) | 2.568(3) | 2.533 | Zr(1)–C(1) | 2.577(3) | 2.542 |
| Zr(1)–C(11) | 2.507(3) | 2.511 | Zr(1)–C(2) | 2.498(3) | 2.514 |
| Zr(1)–C(12) | 2.495(3) | 2.522 | Zr(1)–C(3) | 2.527(2) | 2.515 |
| Zr(1)–C(13) | 2.591(3) | 2.672 | Zr(1)–C(4) | 2.625(2) | 2.667 |
| Zr(1)–C(18) | 2.619(3) | 2.688 | Zr(1)–C(9) | 2.668(3) | 2.675 |
| Zr(1)–Cp°(1) | 2.249 | 2.276 | Zr(1)–Cp°(2) | 2.274 | 2.273 |
| Si(2)–C(12) | 1.870(3) | 1.826 | Si(1)–C(3) | 1.889(3) | 1.821 |
| Si(2)–C(19) | 1.856(3) | 1.885 | Si(1)–C(21) | 1.877(3) | 1.888 |
| Si(2)–C(20) | 1.865(4) | 1.887 | Si(1)–C(22) | 1.874(3) | 1.885 |
| Si(1)–Si(2) | 2.3294(11) | 2.470 |  |  |  |
| *Bond angles* |  |  |  |  |  |
| C(12)–Si(2)–Si(1) | 103.30(9) | 102.57 | C(3)–Si(1)–Si(2) | 102.69(8) | 101.86 |
| C(19)–Si(2)–C(20) | 110.16(18) | 109.91 | C(22)–Si(1)–C(21) | 107.73(17) | 109.68 |
| C(11)–C(12)–Si(2) | 126.8(2) | 123.14 | C(2)–C(3)–Si(1) | 123.1(2) | 125.44 |
| C(13)–C(12)–Si(2) | 127.8(2) | 128.66 | C(4)–C(3)–Si(1) | 131.1(2) | 126.75 |
| Cl(1)–Zr(1)–Cl(2) | 99.18(3) | 102.45 | Cp°(1)–Zr–Cp°(2) | 134.64 | 132.65 |

[a] Cp°, centroid of the Cp mean plane.

Table 4
Comparison of dihedral Cp/Cp, Cp°–Zr–Cp° and Zr–Cp°/Cp angle values for different *rac* and *meso* ansa-bisindenylzirconocene dichlorides

| Compound | Cp/Cp [a] | Cp°–Zr–Cp° [b] | Zr–Cp°/Cp [c] | Ref. |
|---|---|---|---|---|
| *Meso*-Si$_2$Me$_4$(3-SiMe$_3$–Ind)$_2$ZrCl$_2$ | 47.8 | 134.6 | 86.6 | This work |
| *Rac*-C$_2$H$_4$(Ind)$_2$ZrCl$_2$ | 60.4 | 125.3 | 87.2 | [10a] |
| *Meso*-C$_2$H$_4$(Ind)$_2$ZrCl$_2$ | 62.3 | 126.2 | 85.7 | [10b] |
| *Rac*-C$_2$H$_4$(2-$^t$BuMe$_2$SiO–Ind)$_2$ZrCl$_2$ | 58.6 | 125.2 | 88.1 | [10c] |
| *Meso*-C$_2$H$_4$(3-$^t$BuMe$_2$SiOInd)$_2$ZrCl$_2$ | 64.6 | 126.4 | 84.5 | [10d] |
| *Rac*-C$_2$H$_4$(2-NMe$_2$–Ind)$_2$ZrCl$_2$ | n.r. | 127.2 | n.r. | [10e] |
| *Meso*-C$_2$H$_4$(2-NMe$_2$–Ind)$_2$ZrCl$_2$ | n.r. | 127.7 | n.r. | [10f] |

[a] Cp/Cp, dihedral angle between Cp mean planes.
[b] Cp°, centroid of the Cp mean plane.
[c] Zr–Cp°/Cp, angle of the Zr–Cp° axis to the Cp mean plane.

676; $\theta$ range for data collection, 4.70–60.82°; reflections collected, 10 308; independent reflections, 9991 ($R_{int}$ = 0.0326); goodness-of-fit on $F^2$, 1.015; final $R$ indices ($4\sigma$), $R_1$ = 0.0434, $wR_2$ = 0.1023; largest difference peak and hole (e Å$^{-3}$), 0.546 and $-0.521$; structure elucidation by heavy-atom method with SHELXL-87; refinement by full-matrix anisotropic least-squares on $F^2$ with SHELXL-97.

### 3.2. Si$_2$Me$_4$(Ind)$_2$ (**1a**)

Compound **1a** was obtained as described for **1a** from ClSiMe$_2$SiMe$_2$Cl (6.89 g, 36.8 mmol) and IndLi (11.78 g, 95.8 mmol, 30% excess). Exactly 10.46 g of **1a** (yellow solid, 82.0%) were afforded by onefold crystallization of the crude product from hexane at $-30$°C. Anal. Calc. for C$_{22}$H$_{26}$Si$_2$: C, 76.23; H, 7.56; Si, 16.21. Found: C, 75.89; H, 7.22; Si, 16.10%.

$^1$H-NMR (CDCl$_3$, 22°C, $\delta$ ppm): 7.35 (m, 4H), 7.12 (m, 4H), 6.72 (dd, 2H, $J_{HH}$ = 2.2 and 3.6 Hz), 6.30 (dd, 2H, $J_{HH}$ = 0.5 and 3.6 Hz), 3.15 (dd, 2H, $J_{HH}$ = 0.5 and 2.2 Hz), $-0.15$ (s, 6H), $-0.21$ (s, 6H).

### 3.3. Meso-Si$_2$Me$_4$(Ind)$_2$ZrCl$_2$ (**1b**)

Compound **1a** (5.15 g, 14.86 mmol) in ether (100 ml) was metallated with 31 mmol of BuLi (1.6 M hexane solution) at 0°C. After gas release was completed, the formed suspension was filtered, the precipitate was washed with hexane (2 × 40 ml), dried in vacuum and suspended in diethyl ether (100 ml). ClSnMe$_3$ (30 mmol, hexane solution) was added dropwise at room temperature (r.t.), and the mixture was stirred overnight. The solvent was evacuated in vacuum. A 200 ml volume of toluene was added, and the mixture was filtered. ZrCl$_4$ (3.54 g, 15.2 mmol) was added gradually to the solution of the distannylated derivative and it turned orange immediately. The mixture was stirred at r.t. for 48 h and then filtered. The evaporation of the solvent left a dark orange residue which was extracted with hexane in an apparatus of permanent extraction for 18 h. The hexane-insoluble fraction was dried in

vacuum for 2 h, affording 3.09 g (41.0%) of **1b** (yellow powder). Anal. Calc. for C$_{22}$H$_{24}$Cl$_2$Si$_2$Zr: C, 52.15; H, 4.77; Cl, 13.99; Si, 11.09; Zr, 18.00. Found: C, 52.21; H, 4.92; Si, 10.90; Zr, 17.91%. $^1$H-NMR data are listed in Table 1.

Our efforts in separating any individual compound from the hexane-soluble fraction of this synthesis were fruitless. At best, the $^1$H-NMR spectrum of the sample showed up to eight resonances in the area of the SiMe protons.

### 3.4. Si$_2$Me$_4$(2-Me–Ind)$_2$ (**2a**)

Compound **2a** was obtained as described for **1a** from ClSiMe$_2$SiMe$_2$Cl (3.79 g, 20.28 mmol) and 2-Me–IndLi (6.67 g, 48.67 mmol, 20% excess). A 5.22 g sample of **2a** (yellow solid, 68.7%) were afforded by onefold crystallization of crude product from hexane at $-30$°C. Anal. Calc. for C$_{24}$H$_{30}$Si$_2$: C, 76.64; H, 8.07; Si, 14.96. Found: C, 76.95; H, 8.18; Si, 14.72%. $^1$H-NMR (CDCl$_3$, 22°C, $\delta$ ppm): 7.35–7.00 (m, 8H), 6.35 (d, 2H, $J_{HH}$ = 1.0 Hz), 2.9 (d, 2H, $J_{HH}$ = 1.0 Hz), 1.95 (s, 3H), 1.85 (s, 3H), 0.15 (s, 3H), 0.02 (s, 3H), $-0.25$ (s, 3H), $-0.30$ (s, 3H).

### 3.5. Rac- and meso-Si$_2$Me$_4$(2-Me–Ind)$_2$ZrCl$_2$ (**2b**)

Compound **2a** (4.37 g, 11.66 mmol) in ether (100 ml) was metallated with 24 mmol of BuLi (1.6 M hexane solution) at 0°C. After gas release was completed, the formed suspension was filtered, the precipitate was washed with hexane (2 × 40 ml), dried in vacuum and suspended in diethyl ether (100 ml). ClSnMe$_3$ (24.2 mmol, hexane solution) was added dropwise at r.t., and the mixture was stirred overnight. The solvent was evacuated in vacuum. A 200 ml volume of toluene and ZrCl$_4$ (2.7 g, 12.0 mmol) were added gradually to the solution of the distannylated derivative. The mixture was stirred at r.t. for 48 h to form an orange solution with a dark brown oily precipitate. After filtering the

Table 5
Comparison of the stereotactic pentade distribution of elastic PP produced by **2b**/MAO and by (2-PhInd)$_2$ZrCl$_2$/MAO (ether soluble fraction) [13]

| Catalyst | mmmm | mmmr | rmmr | mmrr | mmrm | rmrr + mrmr | rrrr | mrrr | mrrm |
|---|---|---|---|---|---|---|---|---|---|
| Si$_2$Me$_4$(2-MeInd)$_2$ZrCl$_2$ | 0.11 | 0.15 | 0.06 | 0.13 | 0.21 | 0.11 | 0.05 | 0.12 | 0.06 |
| (2-PhInd)$_2$ZrCl$_2$ | 0.18 | 0.16 | 0.06 | 0.12 | 0.22 | 0.11 | 0.03 | 0.07 | 0.05 |

mixture, the evaporation of the solvent left a dark orange residue which was extracted with hexane in an apparatus of permanent extraction for 18 h. The hexane-insoluble fraction was dried in vacuum for 2 h, affording 4.93 g (79.1%) of a 1:1 mixture of *meso*-**2b** and *rac*-**2b** (orange powder). Anal. Calc. for C$_{24}$H$_{28}$Si$_2$Cl$_2$Zr: C, 53.90; H, 5.28; Cl, 13.26; Si, 10.50; Zr, 17.06. Found: C, 54.20; H, 4.99; Si, 10.45; Zr, 17.20%. $^1$H-NMR data are listed in Table 1.

Cooling a solution of the above product in a 9:1 ether-pentane solution at −30°C affords a mixture of *meso*-**2b** and *rac*-**2b** in 3:1 ratio.

### 3.6. Meso-Si$_2$Me$_4$(3-SiMe$_3$–Ind)$_2$ZrCl$_2$ (3b)

Compound **1a** (5.15 g, 14.86 mmol) in ether (100 ml) was metallated with 31 mmol of BuLi (1.6 M hexane solution) at 0°C. After gas release was completed, ClSiMe$_3$ (31 mmol, ether solution) was added dropwise at 0°C. The mixture was stirred overnight and filtered. BuLi (31 mmol, 1.6 M hexane solution) was added dropwise to the solution at 0°C. After gas release was completed, the solvent was evacuated in vacuum. Residual solids were suspended in hexane (100 ml), the suspension was stirred for 1 h and filtered. The precipitate was additionally washed with hexane (2 × 40 ml), dried in vacuum and dissolved in toluene (150 ml). ZrCl$_4$ (3.60 g, 15.3 mmol) was added gradually to the solution at −20°C. The mixture was stirred at r.t. for 48 h and filtered. The evaporation of the solvent left a light orange residue which was extracted with hexane in an apparatus of permanent extraction for 18 h. The volume of hexane-soluble fraction was reduced to 50 ml, and the solution was cooled at −30°C, affording yellow crystals of **3b** (5.08 g, 52.5%). One additional crystallization of the product from hexane at −30°C afforded yellow single crystals of **3b** in 43.1% yield. Anal. Calc. for C$_{28}$H$_{40}$Si$_4$Cl$_2$Zr: C, 51.65; H, 6.19; Cl, 10.89; Si, 17.25; Zr, 14.01. Found: C, 51.78; H, 6.30; Si, 17.24; Zr, 13.91%. $^1$H-NMR data are listed in Table 1.

### 3.7. Meso-Si$_2$Me$_4$(Ind–H$_4$)$_2$ZrCl$_2$ (4)

A 200 ml stainless steel autoclave was charged with **1b** (1.2 g, 2.29 mmol), PtO$_2$ (80 mg), CH$_2$Cl$_2$ (100 ml). The hydrogenation reaction was carried out at 30 atm of H$_2$ at r.t. for 20 h. The solvent was evaporated,

residual solids were extracted with hexane, and the mixture was filtered. Cooling the solution to −60°C gave **4** (white needles) in 25% yield. Anal. Calc. for C$_{22}$H$_{32}$Si$_2$Cl$_2$Zr: C, 51.33; H, 6.27; Cl, 13.77; Si, 10.91; Zr, 17.72. Found: C, 51.34; H, 6.15; Si, 10.60; Zr, 13.98%. $^1$H-NMR data are listed in Table 1.

### 3.8. Polymerization procedure

Propylene polymerizations were carried out in 200 ml glass flasks with vigorous magnetic stirring in toluene (80 ml). The catalysts were preactivated with MAO (Al:Zr = 1000:1) for 20 min. The propylene pressure was maintained at 1 atm upon the polymerization (12 h). The polymerizations were quenched with acidified methanol, the products were washed twice with ethanol and dried in vacuum.

## 4. Supplementary material

Crystallographic data for the structural analysis have been deposited with the Cambridge Crystallographic Data Centre, CSD-116245 for compound *meso*-**3b** and can be obtained from the authors on request.

## References

[1] H.H. Brintzinger, D. Fischer, R. Mülhaupt, B. Rieger, R.M. Waymouth, Angew. Chem. Int. Ed. Engl. 34 (1995) 1143.
[2] For some recent work see: (a) S.C. Yoon, J.-W. Park, H.S. Jung, H. Song, J.T. Park, S.I. Woo, J. Organomet. Chem. 559 (1998) 149. (b) N. Schneider, M.E. Huttenloch, V. Stehling, R. Kirsten, F. Schaper, H.H. Brintzinger, Organometallics 16 (1997) 3413. (c) J.N. Christopher, G.M. Diamond, R.F. Jordan, Organometallics 15 (1996) 4038. (d) J.A. Ewen, A. Zambelli, P. Longo, J.M. Sullivan, Macromol. Rapid Commun. 19 (1998) 71. (e) I. Kim, Macromol. Rapid Commun. 19 (1998) 299. (f) S. Beck, H.H. Brintzinger, J. Suhm, R. Mülhaupt, Macromol. Rapid Commun. 19 (1998) 235. (g) J.C.W. Chien, Y. Iwamoto, M.D. Rausch, W. Wedler, H.H. Winter, Macromolecules 30 (1997) 3447.

[3] (a) P. Jutzi, Y. Mieling, B. Neumann, H.-G. Stammler, J. Organomet. Chem. 541 (1997) 9. (b) P. Jutzi, R. Krallmann, G. Wolf, B. Neumann, H.-G. Stammler, Chem. Ber. 124 (1991) 2391. (c) P. Schertl, H.G. Alt, J. Organomet. Chem. 545 (1997) 553. (d) W. Spaleck, M. Antberg, V. Dolle, J. Rohrmann, A. Winter, New J. Chem. 14 (1990) 499.

[4] (a) I.E. Nifant'ev, P.V. Ivchenko, Organometallics 16 (1997) 713. (b) A.Z. Voskoboynikov, A.Yu. Agarkov, E.A. Chernyshev, I.P. Beletskaya, A.V. Churakov, L.G. Kuz'mina, J. Organomet. Chem. 530 (1997) 75.

[5] (a) SPARTAN, version 5.03, Wave Function Inc., Wave Function Ed., 1998. (b) W.J. Hehre, L.D. Burke, A.J. Shusterman, W.J. Pietro, Experiment in Computation Organic Chemistry, Wave Function Ed., 1995. (c) W.J. Hehre, Practical Strategies for Electronic Structure Calculations, Wave Function De, 1995.

[6] (a) G. Jany, R. Fawzi, M. Steimann, B. Rieger, Organometallics 16 (1997) 544. (b) B. Rieger, G. Jany, Chem. Ber. 127 (1994) 2417.

[7] F.R.W.P. Wild, L. Zsolnai, G. Huttner, H.H. Brintzinger, J. Organomet. Chem. 232 (1982) 233.

[8] K. Schmidt, A. Reinmuth, U. Rief, J. Diebold, H.H. Brintzinger, Organometallics 16 (1997) 1724.

[9] M.S. Erickson, F.R. Fronczek, McLaughlin, J. Organomet. Chem. 415 (1991) 75.

[10] (a) F. Wild, M. Wasiucionek, G. Huttner, H.H. Brintzinger, J. Organomet. Chem. 288 (1985) 63. (b) F. Piemontesi, I. Camurati, L. Resconi, D. Balboni, A. Sironi, M. Moret, R. Zeigler, N. Piccolrovazzi, Organometallics 14 (1995) 1256. (c) R. Leino, H.J.G. Luttikhedde, P. Lehmus, C.-E. Wilén, R. Sjöholm, A. Lehtonen, J.V. Seppälä, J.H. Näsman, Macromolecules 30 (1997) 3477. (d) R. Leino, H.J.G. Luttikhedde, A. Lehtonen, P. Ekholm, J.H. Näsman, J. Organomet. Chem. 558 (1998) 181. (e) H.J.G. Luttikhedde, R.P. Leino, C.-E. Wilén, J.H. Näsman, M.J. Ahlgrén, T.A. Pakkanen, Organometallics 15 (1996) 3092. (f) H.J.G. Luttikhedde, R. Leino, M.J. Ahlgren, T.A. Pakkanen, J.H. Näsman, J. Organomet. Chem. 557 (1998) 227.

[11] From our experience, the calculations on compounds containing silicon atoms fit experimental data better when performed on the AM1 basis set. SPARTAN does not handle transition metal compounds on AM1 level.

[12] J.L. Maciejewski Petoff, R.M. Waymouth, Polym. Prep. Am. Chem. Soc. Div. Polym. Chem. 39 (1998) 212.

[13] E.D. Carlson, M.T. Krejchi, C.D. Shah, T. Terakawa, R.M. Waymouth, G.G. Fuller, Macromolecules 31 (1998) 5343.

[14] (a) S.Ya. Knjazhanski, E.S. Kalyuzhnaya, L.E. Elizalde Herrera, B.M. Bulychev, A.V. Khvostov, A.I. Sizov, J. Organomet. Chem. 531 (1997) 19. (b) S.Ya. Knjazhanski, L. Elizalde, G. Cadenas, B.M. Bulychev, J. Polym. Sci. Pol. Chem. 36 (1998) 1599. (c) S.Ya. Knjazhanski, L. Elizalde, G. Cadenas, B.M. Bulychev, J. Organomet. Chem. 568 (1998) 33.

.